

Effective Crystalline Electric Field Potential in a j - j Coupling Scheme

Takashi HOTTA¹ and Hisatomo HARIMA²

¹Advanced Science Research Center, Japan Atomic Energy Agency, Tokai, Ibaraki 319-1195

²Department of Physics, Faculty of Science, Kobe University, Kobe 657-8501

(Received November 13, 2018)

We propose an effective model on the basis of a j - j coupling scheme to describe local f -electron states for realistic values of Coulomb interaction U and spin-orbit coupling λ , for future development of microscopic theory of magnetism and superconductivity in f^n -electron systems, where n is the number of local f electrons. The effective model is systematically constructed by including the effect of a crystalline electric field (CEF) potential in the perturbation expansion in terms of $1/\lambda$. In this paper, we collect all the terms up to the first order of $1/\lambda$. Solving the effective model, we show the results of the CEF states for each case of $n=2\sim 5$ with O_h symmetry in comparison with those of the Stevens Hamiltonian for the weak CEF. In particular, we carefully discuss the CEF energy levels in an intermediate coupling region with λ/U in the order of 0.1 corresponding to actual f -electron materials between the LS and j - j coupling schemes. Note that the relevant energy scale of U is the Hund's rule interaction. It is found that the CEF energy levels in the intermediate coupling region can be quantitatively reproduced by our modified j - j coupling scheme, when we correctly take into account the corrections in the order of $1/\lambda$ in addition to the CEF terms and Coulomb interactions which remain in the limit of $\lambda=\infty$. As an application of the modified j - j coupling scheme, we discuss the CEF energy levels of filled skutterudites with T_h symmetry.

KEYWORDS: Crystalline electric field, spin-orbit interaction, j - j coupling scheme, LS coupling scheme, filled skutterudites

1. Introduction

Theory of crystalline electric field (CEF) has been developed so far on the basis of an LS coupling scheme.¹⁻³ Nowadays the CEF analysis is reduced to an automatic procedure, since we can simply refer the Hutchings table for CEF parameters,³ B_p^q , depending on the value of total angular momentum J of relevant rare-earth or actinide ion. For instance, for Ce^{3+} ion with one f electron, due to a spin-orbit coupling, the ground state is included in the $J=5/2$ sextet. By consulting the Hutchings table for $J=5/2$,³ we easily find the matrix elements for CEF potential among six states of $J=5/2$. For a cubic system with O_h symmetry, after some algebraic calculations, we immediately understand that the $J=5/2$ sextet is split into Γ_7^- doublet and Γ_8^- quartet.

For the purpose to fit the experimental results on f -electron materials in a high-temperature region, the CEF analysis using the Hutchings table is quite convenient, since it is not necessary to have deep knowledge on the origin of B_p^q , which is given by the sum of electrostatic potentials from the ligand anions surrounding the rare-earth or actinide ion. In fact, for the case of Pr^{3+} ion including two f electrons, it is enough to consider the CEF effect for $J=4$ nonet, which is obtained after the consideration of the Hund's rules and the spin-orbit interaction in the LS coupling scheme. Thus, the competition between CEF effect and Coulomb interactions does not seem to appear in the actual calculation. This fact reduces our task in the CEF analysis.

If f electrons are perfectly localized, we can satisfy with the above treatment and further improvement on the CEF theory may not be required. However, when f -electron properties are gradually changed from localized to itinerant nature, there always appear rich phenomena including exotic magnetism and unconventional superconductivity in f -electron systems. In order to describe the low-energy excitation of f electrons, we should improve the CEF theory so as to be com-

patible with the f -electron Bloch state. For such a purpose, the LS coupling scheme is inconvenient, since the CEF potential is applied to the multi- f -electron state which is firmly constructed from the Hund's rules and the spin-orbit interaction. Rather, a j - j coupling scheme is more convenient, since individual f -electron states are first defined under the effect of CEF potential. Then, we construct the multi- f -electron state by considering the effect of Coulomb interactions, using standard quantum-field theoretical techniques. In contrast, in the LS coupling scheme, we cannot use such standard techniques, since Wick's theorem does not hold.

In order to describe the f -electron system by the Bloch state, it is standard to exploit the relativistic electron band theory, which is based on the j - j coupling scheme. In this sense, it is quite natural to construct an f -electron model on the basis of the j - j coupling scheme. By keeping the same f -electron basis in a simple tight-binding model as that of the relativistic band-structure calculation, we can determine the hopping amplitudes in the tight-binding model to reproduce the Fermi-surface structure of the relativistic band-structure calculation result. After that, we attempt to include electron correlations between f electrons in the tight-binding model.

On the above background, it has been recently proposed to construct a microscopic model for f -electron compounds on the basis of the j - j coupling scheme,^{4,5} by applying a tight-binding approximation for kinetic part of f electrons. Then, microscopic theories have been developed for the understanding of novel magnetism⁶⁻⁹ and unconventional superconductivity¹⁰⁻¹⁵ in f -electron systems. In addition, it is also possible to study complex multipole phenomena from a microscopic viewpoint by using the same f -electron model.¹⁶⁻²¹

However, in the standard j - j coupling scheme in which $j=7/2$ states are simply discarded, only second- and fourth-order CEF parameters (B_2^0 , B_4^0 , and B_4^4) are included. Because of the symmetry reason, the effect of sixth-order terms

(B_6^0 and B_6^2) are dropped. Thus, Γ_3^+ doublet does not appear as a stable ground state in the j - j coupling scheme for O_h symmetry. Moreover, we cannot include the effect of B_6^2 which is characteristic of filled skutterudites with T_h symmetry.²² These points should be improved for the further development of the microscopic theory of f -electron systems on the basis of the j - j coupling scheme.

In this paper, we propose an effective model on the basis of the j - j coupling scheme, which describes low-energy f -electron states by considering the effect of CEF potentials within the first order of $1/\lambda$, where λ is the spin-orbit interaction. Since the effect of sixth-order CEF terms (B_6^0 and B_6^2) are included as two-body potentials for f electrons, we can reproduce the CEF energy levels in the intermediate coupling region on the basis of the concept of the j - j coupling scheme.

The organization of this paper is as follows. In Sec. 2, first we show the local f -electron Hamiltonian H composed of the spin-orbit coupling, the CEF potential, and the Coulomb interactions. On the basis of H , we discuss the f -electron states in the LS and j - j coupling schemes. Then, we derive the effective model from H by the perturbation expansion in terms of $1/\lambda$. In order to compare the results of the effective model with those of the weak CEF region, we also define the Stevens Hamiltonian by the method of operator equivalents.¹ In Sec. 3, we show the results of the effective model for the cases of $n=2\sim 5$ in comparison with those of the Stevens Hamiltonian, where n denotes the local f -electron number. For each n , we compare the CEF energy levels of H_{eff} with those of H in the intermediate coupling region. We also show that the CEF energy levels for T_h symmetry are reproduced in our modified j - j coupling scheme. In Sec. 4, we briefly discuss the f -electron state for $n>7$ in the j - j coupling scheme, by showing the CEF energy levels for the cases of $n=12$ and 13. We remark a couple of future issues concerning the application of our modified j - j coupling schemes. Finally, the paper is summarized. Throughout this paper, we use such units as $\hbar=k_B=1$ and the energy unit is eV.

2. Formulation

2.1 Hamiltonian

In general, the local f -electron Hamiltonian is given by

$$H = H_{\text{so}} + H_{\text{CEF}} + H_{\text{int}}. \quad (1)$$

The first term indicates the spin-orbit coupling, written as

$$H_{\text{so}} = \lambda \sum_{m, \sigma, m', \sigma'} \zeta_{m, \sigma; m', \sigma'} f_{m\sigma}^\dagger f_{m'\sigma'}, \quad (2)$$

where λ is the spin-orbit interaction, $f_{m\sigma}$ is the annihilation operator of f electron, $\sigma=+1$ (-1) for up (down) spin, m is the z -component of angular momentum $\ell=3$, and the matrix elements are expressed by

$$\zeta_{m, \sigma; m, \sigma} = m\sigma/2, \quad \zeta_{m+\sigma, -\sigma; m, \sigma} = \sqrt{\ell(\ell+1) - m(m+\sigma)}/2, \quad (3)$$

and zero for other cases.

The second term denotes the CEF potential, given by

$$H_{\text{CEF}} = \sum_{m, m', \sigma} B_{m, m'} f_{m\sigma}^\dagger f_{m'\sigma}, \quad (4)$$

where $B_{m, m'}$ is determined from the CEF table for $J=\ell=3$.³ Note that electrostatic CEF potentials do not act on f -electron

spin. For the cubic system with O_h symmetry, $B_{m, m'}$ is expressed by two CEF parameters for $J=3$, B_4^0 and B_6^0 , as

$$\begin{aligned} B_{3,3} &= B_{-3,-3} = 180B_4^0 + 180B_6^0, \\ B_{2,2} &= B_{-2,-2} = -420B_4^0 - 1080B_6^0, \\ B_{1,1} &= B_{-1,-1} = 60B_4^0 + 2700B_6^0, \\ B_{0,0} &= 360B_4^0 - 3600B_6^0, \\ B_{3,-1} &= B_{-3,1} = 60\sqrt{15}(B_4^0 - 21B_6^0), \\ B_{2,-2} &= 300B_4^0 + 7560B_6^0. \end{aligned} \quad (5)$$

Note the relation of $B_{m, m'} = B_{m', m}$. Following the traditional notation,² we define

$$B_4^0 = Wx/F(4), \quad B_6^0 = W(1-|x|)/F(6), \quad (6)$$

where x and the sign of W specify the CEF energy scheme, while $|W|$ determines the energy scale for the CEF potential. Concerning non-dimensional parameters, $F(4)$ and $F(6)$, we choose $F(4)=15$ and $F(6)=180$ for $J=3$ by following Ref. 2. In actual f -electron materials, the magnitude of the CEF potential is considered to be $10^{-4}\sim 10^{-3}$ eV. For the calculation of the CEF energy level in this paper, we set $W=-10^{-4}$ eV, even if we do not explicitly mention the value of W .

Finally, H_{int} denotes Coulomb interaction term, given by

$$H_{\text{int}} = \sum_{m_1 \sim m_4, \sigma, \sigma'} I_{m_1 m_2, m_3 m_4} f_{m_1 \sigma}^\dagger f_{m_2 \sigma'}^\dagger f_{m_3 \sigma'} f_{m_4 \sigma}, \quad (7)$$

where the Coulomb integral $I_{m_1 m_2, m_3 m_4}$ is expressed by

$$I_{m_1 m_2, m_3 m_4} = \sum_{k=0}^6 F^k c_k(m_1, m_4) c_k(m_2, m_3). \quad (8)$$

Here F^k is the Slater-Condon parameter^{23,24} and c_k is the Gaunt coefficient^{25,26} which is tabulated in the standard textbooks of quantum mechanics.²⁷ Note that the sum is limited by the Wigner-Eckart theorem to $k=0, 2, 4$, and 6.

In principle, the Slater-Condon parameters and the spin-orbit interaction are determined so as to reproduce the spectra of rare-earth and actinide ions for each value of n , but in any case, the Slater-Condon parameters are considered to be distributed between 1 eV and 10 eV, while λ is in the order of 0.1 eV. In this paper, in order to discuss conveniently the competition between the Coulomb interactions and the spin-orbit coupling, we parameterize F^k as

$$F^0 = 10U, \quad F^2 = 5U, \quad F^4 = 3U, \quad F^6 = U, \quad (9)$$

where U is introduced as a scaling parameter. As long as we set the Slater-Condon parameters between 1 eV and 10 eV, the results obtained in the paper do not change qualitatively, even if we use different values for F^k . As for the meaning of U , roughly speaking, it indicates the order of the Hund's rule interaction J_H among f orbitals, which is considered to be in the order of a few eV. However, for the purpose to explain the change between the LS and j - j coupling schemes, we treat U as a free parameter in the following arguments.

2.2 LS versus j - j coupling schemes

In order to describe the low-energy f^n -electron states of H , there are two typical approaches, the LS coupling and j - j coupling schemes. In the LS coupling scheme, first the total spin \mathbf{S} and total angular momentum \mathbf{L} are formed by following Hund's rules. After forming \mathbf{S} and \mathbf{L} , we include the effect of spin-orbit interaction $\lambda_{LS} \mathbf{L} \cdot \mathbf{S}$, where $\lambda_{LS}=\lambda/n$ for

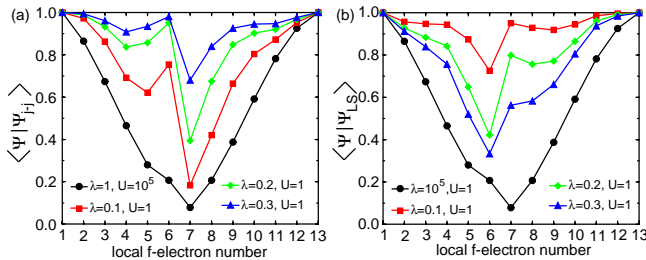


Fig. 1. Overlap integrals (a) $\langle \Psi | \Psi_{j-j} \rangle$ and (b) $\langle \Psi | \Psi_{LS} \rangle$ for $n=1 \sim 13$ for several parameter sets of U and λ .

$n < 7$ and $\lambda_{LS} = -\lambda/(14 - n)$ for $n > 7$. The ground state multiplet is specified by the total angular momentum J , given by $J = L + S$. From simple algebra, the ground-state multiplet is characterized by $J = |L - S|$ for $n < 7$, while $J = L + S$ for $n > 7$.

On the other hand, in the j - j coupling scheme, first we include the spin-orbit coupling so as to define the one-electron state labelled by the total angular momentum j , given by $j = s + \ell$, where s denotes one-electron spin. For f orbitals with $\ell = 3$, we immediately obtain an octet with $j = 7/2 (= 3 + 1/2)$ and a sextet with $j = 5/2 (= 3 - 1/2)$, which are well separated by the spin-orbit interaction. Note here that the level for the octet is higher than that of the sextet. Then, we take into account the effect of Coulomb interactions to accommodate n electrons among the sextet and/or octet, leading to the ground-state level in the j - j coupling scheme. For $n=1 \sim 6$, we accommodate f electrons in the $j = 5/2$ sextet to construct the multiplet specified by J , while for $n=7 \sim 13$, f electrons are accommodated in the $j = 7/2$ octet.

As intuitively understood from the above brief explanation, the LS and j - j coupling schemes become exact in the limit of $U = \infty$ and $\lambda = \infty$, respectively. In actual f -electron materials, as mentioned above, $U (\approx J_H)$ is as large as a few eV. On the other hand, for rare-earth atoms, λ is about $0.1 \sim 0.2$ eV, while it is $0.2 \sim 0.3$ eV for actinide atoms. Thus, the actual situation is characterized by λ/U in the order of 0.1. This intermediate coupling region is close to neither the LS coupling limit ($U = \infty$) and the j - j coupling limit ($\lambda = \infty$), but due to the relation of $U > \lambda$ in actual materials, the LS coupling scheme was widely used for the description of the local f -electron state. Contrary to such a historical trend, we believe that it is meaningful to reexamine the significance of the j - j coupling scheme and to provide an alternative systematic framework to understand the CEF state of f^n -electron compounds.

For the purpose, let us see how the wavefunction of H is changed by U and λ . Here we suppress the CEF potential to focus on the competition between the Coulomb interaction and the spin-orbit coupling. In Fig. 1(a), we depict the overlap integral $\langle \Psi | \Psi_{j-j} \rangle$ for $n=1 \sim 13$ for several sets of λ and U , where $|\Psi\rangle$ is the ground state of $H_{\text{so}} + H_{\text{int}}$ and $|\Psi_{j-j}\rangle$ denotes the state at the limit of $\lambda = \infty$. Here we use $\lambda = 10^5$ and $U = 1$ to express virtually the j - j coupling limit. The solid circles denote the overlap integral between the LS and j - j coupling schemes, $\langle \Psi_{LS} | \Psi_{j-j} \rangle$, where $|\Psi_{LS}\rangle$ denotes the state at the LS coupling limit. Note that we set $\lambda = 1$ and $U = 10^5$, where U is large enough to arrive at the LS coupling limit. We find that $\langle \Psi_{LS} | \Psi_{j-j} \rangle$ exhibits a “V”-shaped function of n . It is natural, since the Hund’s rule interaction works most

effectively at half filling ($n=7$), which is the worst case for the j - j coupling scheme.

In the intermediate coupling region for $\lambda = 0.1 \sim 0.3$ and $U = 1$, the overlap integrals are increased with the increase of λ . In particular, for $n < 7$ and $\lambda = 0.1$, the values of $\langle \Psi | \Psi_{j-j} \rangle$ are larger than 0.6. This lower limit becomes 0.8 and 0.9 for $\lambda = 0.2$ and 0.3, respectively. These facts suggest that the j - j coupling scheme is the good starting approximation to consider the f^n -electron state for $n < 7$.

Note that the values of $\langle \Psi | \Psi_{j-j} \rangle$ for $n = 5$ and 6 become larger than that for $n = 4$, leading to a shallow minimum around at $n = 3 \sim 4$, when λ is increased. It is intuitively understood by the electron-hole relation among the $j = 5/2$ sextet in the j - j coupling scheme. For $n = 6$, the singlet ($J = 0$) of fully occupied $j = 5/2$ state is considered to be very stable, since it is the closed-shell structure in the j - j coupling scheme. For $n = 5$, when we accommodate five f electrons in the $j = 5/2$ sextet, it corresponds to the one-hole case. In the j - j coupling limit, we expect that the wavefunction for one-hole state is the same as that of one-electron case due to the electron-hole conversion. Thus, the overlap integral is rather increased for $n = 5$ and 6, in comparison with the case of $n = 4$, when we increase λ . This fact also supports that we can construct the ground state in the intermediate coupling region on the basis of the j - j coupling scheme. Note that for $n \geq 7$, the overlap integral is also increased with the increase of λ and n . In the region of $n \geq 8$, the values seem to approach unity gradually, but for $n = 7$, it is increased only slowly. For the half-filling case, it is difficult to recommend the usage of the j - j coupling scheme.

In Fig. 1(b), we show the overlap integral with the LS coupling wavefunction, defined by $\langle \Psi | \Psi_{LS} \rangle$, for $n = 1 \sim 13$ for several sets of λ and U . The solid circles are the same as those in Fig. 1(a), since they denote $\langle \Psi_{j-j} | \Psi_{LS} \rangle$. For $\lambda = 0.1$ and $U = 1$, the ground state of H is well approximated by the LS coupling state except for $n = 6$, since we find $\langle \Psi | \Psi_{j-j} \rangle > 0.9$ for $n = 1 \sim 5$ and $7 \sim 13$. When we increase λ , the overlap integrals are totally suppressed. For $\lambda = 0.3$, it seems to be difficult to use the LS coupling scheme, in particular, for the region near $n = 6$.

In order to construct an effective model in the intermediate coupling region with λ/U in the order of 0.1, it is necessary to improve one of the LS and j - j coupling schemes. We prefer one of the schemes, depending on the nature of the current problem. For $n \leq 6$ and $n \geq 8$, we believe that the j - j coupling scheme provides us the good starting point to approach the intermediate coupling region. As mentioned in the introduction, it is difficult to include the itinerant nature of f electrons in the LS coupling scheme. In order to describe the Bloch state of f electron, we should prefer the j - j coupling scheme for the description of the f -electron state. Then, we consider the local f -electron problem to construct the effective model by the perturbation expansion in terms of $1/\lambda$ from the limit of $\lambda = \infty$.

In the j - j coupling scheme, even if we include the effect of the order of $1/\lambda$, the local f -electron state is still composed of the $j = 5/2$ sextet. When the periodic system is discussed by using the effective model constructed from the $j = 5/2$ states, we consider the hybridization between $j = 5/2$ states and conduction bands, although in actuality, there should also exist the hybridization of $j = 7/2$ states. However, in the relativistic band-structure calculations for light rare-earth materials,

the $j=5/2$ sextet is occupied, while the $j=7/2$ octet is unoccupied, suggesting that f electrons in the $j=5/2$ sextet mainly contribute to the ground and the low-energy excited states. In fact, the Fermi-surface sheets are composed of $j=5/2$ electrons. Since we are interested in the electronic structure near the Fermi level, it seems natural to exploit the $j=5/2$ states for the construction of the effective model to discuss low-energy electronic properties of f -electron materials.

2.3 Effective model due to the expansion in terms of $1/\lambda$

Now let us construct the effective Hamiltonian in the j - j coupling scheme by including the effect of the CEF potentials in the perturbation expansion in terms of $1/\lambda$. Note that the energy scale $|W|$ of the CEF potential is much smaller than U and λ . As already mentioned, we set $W=-10^{-4}$ eV in this paper to be consistent with such a situation of the weak CEF.

First we transform the f -electron basis between (m, σ) and (j, μ) representations, connected by Clebsch-Gordan coefficients, where j is the total angular momentum and μ is the z -component of j . Hereafter we use symbols “ a ” and “ b ” for $j=5/2$ and $7/2$, respectively. When we define $f_{j\mu}$ as the annihilation operator for f electron labeled by j and μ , the transformation is defined as

$$f_{j\mu} = \sum_{m,\sigma} C_{j,\mu;m,\sigma} f_{m\sigma}, \quad (10)$$

where the Clebsch-Gordan coefficient $C_{j,\mu;m,\sigma}$ is given by

$$\begin{aligned} C_{a,\mu;\mu-\sigma/2,\sigma} &= -\sigma\sqrt{(7/2-\sigma\mu)/7}, \\ C_{b,\mu;\mu-\sigma/2,\sigma} &= \sqrt{(7/2+\sigma\mu)/7}, \end{aligned} \quad (11)$$

and other components are zero.

After the transformation, we express H as

$$H = H_{\text{so}} + H', \quad (12)$$

where the spin-orbit coupling term H_{so} is diagonalized as

$$H_{\text{so}} = \sum_{j,\mu} \lambda_j f_{j\mu}^\dagger f_{j\mu}, \quad (13)$$

with $\lambda_a=-2\lambda$ and $\lambda_b=(3/2)\lambda$. The remaining part includes the CEF and Coulomb interaction terms as

$$H' = H_{\text{CEF}} + H_{\text{int}}, \quad (14)$$

where H_{CEF} and H_{int} are given by

$$H_{\text{CEF}} = \sum_{j_1\mu_1, j_2\mu_2} \tilde{B}_{\mu_1\mu_2, \mu_3\mu_4}^{j_1, j_2} f_{j_1\mu_1}^\dagger f_{j_2\mu_2}, \quad (15)$$

and

$$H_{\text{int}} = \sum_{j_1 \sim j_4} \sum_{\mu_1 \sim \mu_4} \tilde{I}_{\mu_1\mu_2, \mu_3\mu_4}^{j_1, j_2, j_3, j_4} f_{j_1\mu_1}^\dagger f_{j_2\mu_2}^\dagger f_{j_3\mu_3} f_{j_4\mu_4}, \quad (16)$$

respectively. Note that \tilde{B} and \tilde{I} are the CEF potential and Coulomb interactions expressed in the basis of j and μ .

In order to obtain the effective model, we use the degenerate perturbation theory by treating H' as a perturbation to H_{so} . The effective model is written as

$$H_{\text{eff}} = H_a^{(0)} + H_a^{(1)}, \quad (17)$$

where $H_j^{(k)}$ denotes the k th-order term with respect to $1/\lambda$ for the multiplet labeled by j . The zeroth-order term $H_a^{(0)}$ indicates the model in the standard j - j coupling scheme.^{4,5}

When we simply ignore all the terms including the symbol b ($j=7/2$), we obtain $H_a^{(0)}$ as

$$H_a^{(0)} = H_{\text{CEF}}^{(0)} + H_{\text{int}}^{(0)}. \quad (18)$$

The CEF term is given by

$$H_{\text{CEF}}^{(0)} = \sum_{\alpha_1, \alpha_2} \tilde{B}_{\alpha_1, \alpha_2}^{a,a} f_{a\alpha_1}^\dagger f_{a\alpha_2}, \quad (19)$$

where $\tilde{B}_{\alpha_1, \alpha_2}^{a,a}$ denotes the CEF potential for $J=5/2$, given by

$$\begin{aligned} \tilde{B}_{\pm 5/2, \pm 5/2}^{a,a} &= 60B_4^0(1, 5/2), \\ \tilde{B}_{\pm 3/2, \pm 3/2}^{a,a} &= -180B_4^0(1, 5/2), \\ \tilde{B}_{\pm 1/2, \pm 1/2}^{a,a} &= 120B_4^0(1, 5/2), \\ \tilde{B}_{\pm 5/2, \mp 3/2}^{a,a} &= B_{\mp 3/2, \pm 5/2} = 60\sqrt{5}B_4^0(1, 5/2). \end{aligned} \quad (20)$$

Here $B_4^0(n, J)$ denotes the CEF parameter for n and J , where n is the local f -electron number and J denotes the total angular momentum of ground state multiplet. For $n=1$ and $J=5/2$, $B_4^0(1, 5/2)$ is related with B_4^0 for $J=\ell=3$ in eq. (6) as

$$B_4^0(1, 5/2) = (11/7)B_4^0. \quad (21)$$

The meaning of the coefficient 11/7 will be explained later.

The Coulomb interaction term is given by

$$H_{\text{int}}^{(0)} = \sum_{\alpha_1 \sim \alpha_4} \tilde{I}_{\alpha_1\alpha_2, \alpha_3\alpha_4}^{aa,aa} f_{a\alpha_1}^\dagger f_{a\alpha_2}^\dagger f_{a\alpha_3} f_{a\alpha_4}, \quad (22)$$

where the Coulomb integral $\tilde{I}^{aa,aa}$ is expressed by three Racah parameters, E_0 , E_1 , and E_2 ,^{4,5} which are related to the Slater-Condon parameters as

$$\begin{aligned} E_0 &= F^0 - (80/1225)F^2 - (12/441)F^4, \\ E_1 &= (120/1225)F^2 + (18/441)F^4, \\ E_2 &= (12/1225)F^2 - (1/441)F^4. \end{aligned} \quad (23)$$

Among Coulomb interactions, the Hund's rule coupling is the relevant energy scale for the construction of multi- f -state. In this case, among three Racah parameters, E_2 plays a role of the Hund's rule coupling in the j - j coupling scheme. Concerning the magnitude, by combining eqs. (9) and (23), we obtain $E_2=(31/15)U/49=0.04U$ in the present parameterization. Note that the magnitude of the Hund's rule interaction in the j - j coupling scheme is generally reduced. In order to understand this point intuitively, it is convenient to consider a simple Hund's rule term, expressed as $-J_H s^2$, where s denotes the spin of f electron. Here we note the relation $s=(g_J-1)\mathbf{j}$, where g_J is the Landé's g -factor and \mathbf{j} indicates the total angular momentum. Since $g_J=6/7$ for $j=5/2$, we obtain $s=-(1/7)\mathbf{j}$. Namely, the original Hund's rule term is rewritten as $-(J_H/49)\mathbf{j}^2$ in the j - j coupling scheme. Thus, the Hund's rule interaction in the j - j coupling scheme is reduced as $J_H/49$ from the original value. As discussed later, this reduction has an important meaning to understand the rather wide applicability of the effective model.

Now we consider the correction term in the order of $1/\lambda$, which is written as

$$H_a^{(1)} = H_{\text{CEF}}^{(1)} + H_{\text{int}}^{(1)}. \quad (24)$$

The CEF term is given by

$$H_{\text{CEF}}^{(1)} = \sum_{\alpha_1, \alpha_2} \tilde{B}_{\alpha_1, \alpha_2}^{(1)} f_{a\alpha_1}^\dagger f_{a\alpha_2}, \quad (25)$$

with

$$\tilde{B}_{\alpha_1, \alpha_2}^{(1)} = \sum_{\beta} \frac{\langle \alpha_1 | H_{\text{CEF}} | \beta \rangle \langle \beta | H_{\text{CEF}} | \alpha_2 \rangle}{\lambda_a - \lambda_b}, \quad (26)$$

where $|\alpha\rangle = f_{a\alpha}^\dagger |0\rangle$ and $|\beta\rangle = f_{b\beta}^\dagger |0\rangle$. For O_h symmetry, after some algebraic calculations, we obtain

$$\begin{aligned} \tilde{B}_{5/2, 5/2}^{(1)} &= \tilde{B}_{-5/2, -5/2}^{(1)} = 5\varepsilon_8/6 + \varepsilon_7/6, \\ \tilde{B}_{3/2, 3/2}^{(1)} &= \tilde{B}_{-3/2, -3/2}^{(1)} = \varepsilon_8/6 + 5\varepsilon_7/6, \\ \tilde{B}_{1/2, 1/2}^{(1)} &= \tilde{B}_{-1/2, -1/2}^{(1)} = \varepsilon_8, \\ \tilde{B}_{5/2, -3/2}^{(1)} &= \tilde{B}_{3/2, -5/2}^{(1)} = \sqrt{5}(\varepsilon_8 - \varepsilon_7)/6, \end{aligned} \quad (27)$$

where ε_7 and ε_8 are, respectively, given by

$$\varepsilon_7 = -\left(\frac{240}{7}\right)^2 \frac{6}{7\lambda} (5B_4^0 + 126B_6^0)^2, \quad (28)$$

and

$$\varepsilon_8 = -\left(\frac{720}{7}\right)^2 \frac{10}{7\lambda} (B_4^0 - 21B_6^0)^2. \quad (29)$$

These values indicate the energy corrections for Γ_7^- and Γ_8^- states at $n=1$, respectively. Note that such corrections are in the order of W^2/λ , as easily understood from the definition of $\tilde{B}_{\alpha_1, \alpha_2}^{(1)}$.

Concerning the $1/\lambda$ -correction to the two-body potential, $H_{\text{int}}^{(1)}$ is expressed as

$$H_{\text{int}}^{(1)} = \sum_{\alpha_1 \sim \alpha_4} \tilde{I}_{\alpha_1 \alpha_2, \alpha_3 \alpha_4}^{(1)} f_{a\alpha_1}^\dagger f_{a\alpha_2}^\dagger f_{a\alpha_3} f_{a\alpha_4}, \quad (30)$$

where the two-body potential is formally given by

$$\begin{aligned} \tilde{I}_{\alpha_1 \alpha_2, \alpha_3 \alpha_4}^{(1)} &= \sum_{\alpha, \beta} \frac{\langle \alpha_1 \alpha_2 | H' | \alpha \beta \rangle \langle \beta \alpha | H' | \alpha_3 \alpha_4 \rangle}{\lambda_a - \lambda_b} \\ &+ \sum_{\beta_1, \beta_2} \frac{\langle \alpha_1 \alpha_2 | H' | \beta_1 \beta_2 \rangle \langle \beta_2 \beta_1 | H' | \alpha_3 \alpha_4 \rangle}{2(\lambda_a - \lambda_b)} \\ &- \langle \alpha_1 \alpha_2 | H_{\text{CEF}}^{(1)} | \alpha_3 \alpha_4 \rangle, \end{aligned} \quad (31)$$

where $|\alpha_1 \alpha_2\rangle = f_{a\alpha_1}^\dagger f_{a\alpha_2}^\dagger |0\rangle$, $|\alpha \beta\rangle = f_{a\alpha}^\dagger f_{b\beta}^\dagger |0\rangle$, and $|\beta_1 \beta_2\rangle = f_{b\beta_1}^\dagger f_{b\beta_2}^\dagger |0\rangle$. Note that the final term in eq. (31) is needed to avoid the double-count of the contributions from $H_{\text{CEF}}^{(1)}$, when we diagonalize H_{eff} for $n \geq 2$. As we will see later, the two-body effective potential $\tilde{I}^{(1)}$ plays a crucial role in the intermediate coupling region. It may be possible to obtain the analytic form of $\tilde{I}^{(1)}$ after lengthy and tedious algebraic calculations, but in this paper, we evaluate $\tilde{I}^{(1)}$ only numerically, since our purpose here is to show that H_{eff} actually works. The derivation of more convenient analytic form of $\tilde{I}^{(1)}$ is one of future tasks.

Now we discuss the range of the value of λ , in which H_{eff} works. First we note that $H_{\text{CEF}}^{(1)}$ is in the order of W^2/λ . Since this term is small in the order of $|W|/\lambda$ in comparison with $H_{\text{CEF}}^{(0)}$, it does not play important roles. The first two terms in eq. (31) also include the contributions in the order of W^2/λ , but we find that they are exactly cancelled by the last term. Thus, the lowest contribution to the CEF potential from $H_{\text{int}}^{(1)}$ is in the order of $|W|U/\lambda$. Note that the terms in the order of U^2/λ are not important, since they contribute to the energy shift of the ground-state multiplet.

From the mathematical viewpoint of the convergence of the perturbation expansion, $|W|U/\lambda$ is thought to be smaller than $|W|$, which is the energy scale of $H_{\text{CEF}}^{(0)}$. Namely, we obtain the condition of $U/\lambda \ll 1$, but under this condition, H_{eff} cannot be used for realistic systems at the first glance, since U is larger than λ in f -electron compounds. In order to reconsider this point, we note that the sixth-order contributions of the CEF potential first appear in $H_{\text{CEF}}^{(1)}$ in the order of $|W|U/\lambda$. Since it is enough for us to keep the condition of the weak CEF, $|W|U/\lambda$ should be smaller than the relevant energy scale of $H_{\text{int}}^{(0)}$, i.e., the Hund's rule interaction in the j - j coupling scheme. Thus, we obtain another realistic condition of $|W|U/\lambda \ll E_2$. Here we note that the right-hand side is E_2 , not U . On the other hand, in the left-hand side, U is needed, since all the Coulomb interaction terms contribute to eq. (31) in the intermediate processes. From eqs. (9) and (23), we obtain the revised condition of $|W|/\lambda \ll 0.04$ in the present parameter choice. In comparison with one of the original conditions of the weak CEF ($|W|/\lambda \ll 1$), the range of λ in which H_{eff} works seems to be narrow, but when we compare the condition of $|W|/\lambda \ll 0.04$ with that of $U/\lambda \ll 1$, we understand that the range of λ becomes wide so as to include the realistic parameter space. For instance, for the case of $|W|=10^{-4}$ eV, it is allowed to take λ in the order of 0.1 eV, which is the realistic value for rare-earth ion.

2.4 Stevens Hamiltonian in the weak CEF

In the previous subsection, we have set the effective model H_{eff} due to the expansion in terms of $1/\lambda$ from the limit of $\lambda=\infty$. In order to assess the applicability of the effective model from the quantitative viewpoint, it is necessary to compare the results of H_{eff} with those of H . For the purpose, in addition to the direct comparison between H and H_{eff} , it is useful to introduce the CEF Hamiltonian for O_h symmetry in the region of weak CEF, since we always consider the case of $U \gg |W|$ and $\lambda \gg |W|$. The CEF Hamiltonian is conventionally expressed by using the method of Stevens' operator equivalent as¹

$$H_S = B_4^0(n, J)(\hat{O}_4^0 + 5\hat{O}_4^4) + B_6^0(n, J)(\hat{O}_6^0 - 21\hat{O}_6^4), \quad (32)$$

where $B_p^q(n, J)$ and \hat{O}_p^q denote, respectively, the CEF parameter and the Stevens' operator equivalent for n and J . We call H_S the Stevens Hamiltonian. The matrix elements of \hat{O}_p^q for any value of J have been tabulated by Hutchings.³ Here we explicitly show the values of n and J in the parentheses of the CEF parameter, in order to distinguish them from B_4^0 and B_6^0 for $J=\ell=3$ in eq. (6). Note that H_S is the effective Hamiltonian for the multiplet specified by J for any values of U and λ , as long as they are much larger than $|W|$. In fact, we have checked that the energy levels of H are correctly reproduced by H_S with satisfactory precision for $U(\gg |W|)$ and $\lambda(\gg |W|)$, except for the case of $n=3$ and $\lambda=\infty$.

Effects of U and λ appear in the CEF parameters, $B_4^0(n, J)$ and $B_6^0(n, J)$, which are expressed by

$$B_4^0(n, J) = A_4 \langle r^4 \rangle \beta_J^{(n)}, \quad B_6^0(n, J) = A_6 \langle r^6 \rangle \gamma_J^{(n)}, \quad (33)$$

where A_k is the parameter depending on materials, $\beta_J^{(n)}$ and $\gamma_J^{(n)}$ are the so-called Stevens factors, which are coefficients appearing in the method of Stevens' operator equivalent,¹

n	J	$k_4(n, J)$		$k_6(n, J)$	
		LS	j-j	LS	j-j
1	5/2	11/7	11/7	0	0
2	4	-2/11	-11/49	-68/1155	0
3	9/2	-340/4719	0	1615/44044	0
4	4	476/4719	11/49	-646/11011	0
5	5/2	13/21	-11/7	0	0

Table I. Coefficients $k_4(n, J)$ and $k_6(n, J)$ for $n=1\sim 5$ both in the LS and j-j coupling schemes.

and $\langle r^k \rangle$ denotes the radial average of local f -electron wavefunction. Note that in general, $\beta_J^{(n)}$ and $\gamma_J^{(n)}$ depend on the Coulomb interaction and spin-orbit coupling, since they are determined by the nature of the ground-state multiplet specified by J . In the present paper, the CEF potentials are always given by B_4^0 and B_6^0 . Thus, we express $B_4^0(n, J)$ and $B_6^0(n, J)$ as

$$B_4^0(n, J) = k_4(n, J)B_4^0, \quad B_6^0(n, J) = k_6(n, J)B_6^0. \quad (34)$$

By assuming that A_k and $\langle r^k \rangle$ are not changed in the same material group, we obtain

$$k_4(n, J) = \beta_J^{(n)} / \beta_\ell, \quad k_6(n, J) = \gamma_J^{(n)} / \gamma_\ell, \quad (35)$$

where β_ℓ and γ_ℓ for one f electron with $\ell=3$ are given by¹

$$\beta_\ell = 2/(45 \cdot 11), \quad \gamma_\ell = -4/(9 \cdot 13 \cdot 33), \quad (36)$$

respectively.

First let us consider the limit of $U=\infty$, i.e., the LS coupling scheme. We easily obtain $k_4(n, J)$ and $k_6(n, J)$ due to simple algebraic calculations by using the values of $\beta_J^{(n)}$ and $\gamma_J^{(n)}$ for the LS coupling scheme.¹ For $n=1$ and $J=5/2$, from $\beta_{5/2}^{(1)}=2/(45 \cdot 7)$, we easily obtain

$$k_4^{LS}(1, 5/2) = 11/7, \quad (37)$$

as shown in eq. (21). For $n=2$ and $J=4$, we find

$$\begin{aligned} k_4^{LS}(2, 4) &= \beta_4^{(2)} / \beta_\ell = -2/11, \\ k_6^{LS}(2, 4) &= \gamma_4^{(2)} / \gamma_\ell = -68/1155. \end{aligned} \quad (38)$$

We can obtain $k_4^{LS}(n, J)$ and $k_6^{LS}(n, J)$ for $n \geq 3$, as shown in Table I.

Next we consider another limit of $\lambda=\infty$, i.e., the j-j coupling scheme. As long as we consider the situation of the weak CEF, it is possible to obtain the CEF energy levels by using the Stevens Hamiltonian H_S , even in the limit of $\lambda=\infty$, provided that $B_4^0(n, J)$ and $B_6^0(n, J)$ are correctly evaluated. First we remark a couple of issues which can be understood without calculations: (i) Since B_6^0 does not appear in the j-j coupling scheme due to the symmetry reason, we always obtain $k_6^{j-j}(n, J)=0$ for $n < 7$ in the j-j coupling limit. (ii) For $n=1$, $k_4^{j-j}(1, 5/2)$ is equal to $k_4^{LS}(1, 5/2)$.

Concerning $k_4(n, J)$ for $n=2\sim 5$ in the j-j coupling limit, we evaluate the value in the following procedure: Let us consider the case of $n=2$ as a typical example. We note $|2, 4, 4\rangle = f_{a, 5/2}^\dagger f_{a, 3/2}^\dagger |0\rangle$ in the j-j coupling scheme, where $|n, J, J_z\rangle$ generally denotes the eigenstate determined by $H_{\text{so}}+H_{\text{int}}$, J_z is the z component of total angular momentum J , and $|0\rangle$ is the vacuum state. In the j-j coupling scheme, $|n, J, J_z\rangle$ for $n \leq 6$ indicates the eigenstate of $H_{\text{int}}^{(0)}$. Note that

the bra vector is defined as $\langle n, J, J_z |$. Then, we evaluate the CEF matrix element as

$$\langle 2, 4, 4 | H_{\text{CEF}}^{(0)} | 2, 4, 4 \rangle = -120B_4^0(1, 5/2) = -(1320/7)B_4^0, \quad (39)$$

from eqs. (20) and (21). Since the same matrix element is given by $840B_4^0(2, 4)$ from the Hutchings table,³ we obtain

$$k_4^{j-j}(2, 4) = -11/49, \quad (40)$$

in the j-j coupling limit for $n=2$ and $J=4$. Also for $n=3\sim 5$, we can evaluate $k_4^{j-j}(n, J)$ in the similar way and the results are listed in Table I. It should be noted that $k_4^{j-j}(3, 9/2)=0$. Since $|3, 9/2, 9/2\rangle = f_{a, 5/2}^\dagger f_{a, 3/2}^\dagger f_{a, 1/2}^\dagger |0\rangle$, we easily find $\langle 3, 9/2, 9/2 | H_{\text{CEF}}^{(0)} | 3, 9/2, 9/2 \rangle = 0$. Namely, for $n=3$ and $J=9/2$, the lowest-order contribution of the CEF potential is in the order of W^2 , not in the order of W , in the j-j coupling scheme. This point will be discussed later again.

For the intermediate coupling region in which both U and λ are finite, we evaluate numerically $k_4(n, J)$ and $k_6(n, J)$ by deriving H_S from the original Hamiltonian H . First we diagonalize $H_{\text{so}}+H_{\text{int}}$ as

$$(H_{\text{so}}+H_{\text{int}})|n, J, J_z\rangle = E(n, J)|n, J, J_z\rangle. \quad (41)$$

Note that the ground state has $(2J+1)$ -fold degeneracy, when the CEF potential is ignored. Then, we consider the CEF potential of O_h symmetry in the first order of W and the Hamiltonian H_S is expressed in the matrix form as

$$H_S(J_z, J'_z) = \langle n, J, J_z | H_{\text{CEF}} | n, J, J'_z \rangle. \quad (42)$$

Since the matrix elements of H_S have been already listed for each value of J by using $B_4^0(n, J)$ and $B_6^0(n, J)$,³ we can numerically obtain $B_4^0(n, J)$ and $B_6^0(n, J)$ from eq. (42) for any values of U and λ for a given value of n .

For comparison, we also evaluate $B_4^0(n, J)$ and $B_6^0(n, J)$ from H_{eff} . In this case, the procedure is almost the same as above. First we diagonalize H_{eff} at $W=0$ as

$$H_{\text{eff}}(W=0)|n, J, J_z\rangle = E_{\text{eff}}(n, J)|n, J, J_z\rangle. \quad (43)$$

Then, the Hamiltonian H_S^{eff} from H_{eff} for small W is expressed in the matrix form as

$$\begin{aligned} H_S^{\text{eff}}(J_z, J'_z) &= \langle n, J, J_z | H_{\text{eff}}(W) | n, J, J'_z \rangle \\ &\quad - E_{\text{eff}}(n, J) \delta_{J_z, J'_z}. \end{aligned} \quad (44)$$

In order to obtain $B_4^0(n, J)$ and $B_6^0(n, J)$ numerically, we compare the matrix elements of eq. (44) with the table of Hutchings.

3. Results

3.1 f^2 states

First we explain the case of $n=2$ in detail. Before proceeding to the result of H_{eff} for $n=2$, let us examine the results of the LS and j-j coupling schemes. Then, readers can understand how the j-j coupling scheme will be improved by H_{eff} . In Figs. 2(a) and 2(b), we show the CEF energy levels obtained by the direct diagonalization of H for $(U, \lambda)=(10^5, 1)$ and $(1, 10^5)$, which correspond to the LS and the j-j coupling limits, respectively. Note that the origin of the energy is appropriately shifted for convenience.

In Fig. 2(a), the situation corresponds to the LS coupling scheme, in which first we obtain the ground-state level as 3H

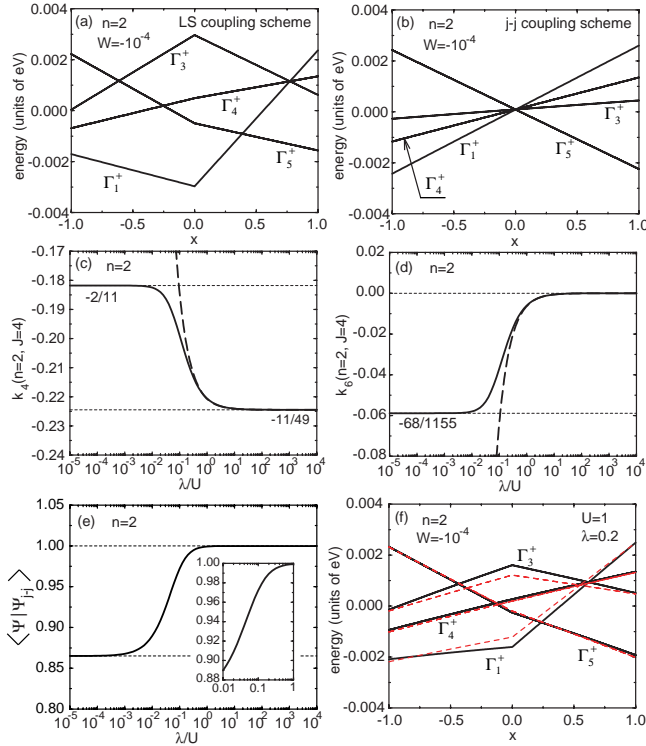


Fig. 2. (a) CEF energy levels in the LS coupling scheme for $n=2$. We diagonalize H for $U=10^5$ and $\lambda=1$. (b) CEF energy levels in the j - j coupling scheme for $n=2$. Here we set $U=1$ and $\lambda=10^5$ for H . (c) $k_4(2,4)$ and (d) $k_6(2,4)$ as functions of λ/U for $n=2$. Broken curves denote $k_4(2,4)$ and $k_6(2,4)$ evaluated from H_{eff} . (e) Overlap integral $\langle \Psi | \Psi_{j-} \rangle$ as a function of λ/U for $n=2$. Inset indicates the result in the intermediate coupling region in a magnified scale. The overlap is evaluated by the diagonalization of $H_{\text{so}} + H_{\text{int}}$. (f) CEF energy levels of H_{eff} (black solid curves) and those of H (red broken curves) for $n=2$, $U=1$, and $\lambda=0.2$.

with $S=1$ and $L=5$ due to the Hund's rules in f shells. Upon further including the spin-orbit interaction, the ground state is specified by $J=4$ expressed as 3H_4 in the traditional notation. After considering the CEF potential, we find nine eigen states, Γ_1^+ singlet, Γ_3^+ doublet, and two kinds of triplets (Γ_4^+ and Γ_5^+).² It is found that the eigen energies of H_S for $n=2$ and $J=4$ agree perfectly with those in Fig. 2(a), when we use $k_4^{LS}(2,4)$ and $k_6^{LS}(2,4)$ in Table I.

In Fig. 2(b), we show the results of H in the limit of the j - j coupling scheme. We have checked that these CEF energies are the same as those of $H_a^{(0)}$ for $n=2$. Note that the results seem to be different from those in Ref. 4 at the first glance, but it is simply due to the negative sign of W . As mentioned in the previous section, even for the j - j coupling scheme, as long as we consider the situation of the weak CEF, it is possible to obtain the CEF energy levels by using the Stevens Hamiltonian H_S . We obtain the same results as those in Fig. 2(b) by diagonalizing H_S with $B_4^0(2,4)=-(11/49)B_4^0$ and $B_6^0(2,4)=0$.

The energy levels in Fig. 2(b) can be understood more intuitively as follows. In the limit of $\lambda=\infty$, the effective model H_{eff} is simply reduced to $H_a^{(0)}$, in which the only relevant CEF parameter is B_4^0 , leading to the splitting between Γ_7^- and Γ_8^- levels for $n=1$. Thus, we obtain the eigen states for $n=2$ by accommodating a couple of electrons in the potential for $n=1$. For $x<0$ with positive B_4^0 , we find the Γ_1^+ singlet ground state, including doubly occupied Γ_7^- orbitals, since Γ_7^- dou-

blet is the ground state for $n=1$ in the region of $x<0$. The first excited state is Γ_4^+ triplet, which is formed by Γ_7^- and Γ_8^- electrons. For $x>0$, since the ground state for $n=1$ is the Γ_8^- quartet, the ground state for $n=2$ is Γ_5^+ triplet composed of a couple of Γ_8^- electrons, stabilized by the Hund's rule interaction. The first excited state in this region is Γ_3^+ doublet, which contains the component of a couple of Γ_8^- electrons.

It is true that all the states appearing in the LS coupling scheme can be also found in the j - j coupling scheme. In particular, at $x=\pm 1$, the CEF energy levels agree well with those in Fig. 2(a). However, when we compare Figs. 2(a) and 2(b) in the region of $|x|\neq 1$, the j - j coupling results seem to be different from those of the LS coupling scheme, since the effect of B_6^0 is not included, as already mentioned in the introduction and in Ref. 4. This is quite natural, if we recall the fact that there exist no contributions of B_6^0 in the Hutchings table for $J=5/2$. This point is improved when we consider the $1/\lambda$ corrections, as shown later.

In Figs. 2(c) and 2(d), we show $k_4(2,4)$ and $k_6(2,4)$, respectively, as functions of λ/U . Since the results have been found to depend only on the ratio of λ/U , we change λ and U appropriately by keeping the condition of the weak CEF, i.e., $\lambda \gg |W|$ and $U \gg |W|$. In actual calculations, for $\lambda/U \geq 1$, we gradually increase λ from unity by setting $U=1$, while for $\lambda/U \leq 1$, U is increased from unity for the fixed value of $\lambda=1$. Both in the limits of $\lambda/U=0$ (LS coupling scheme) and $\lambda/U=\infty$ (j - j coupling scheme), the numerical results correctly approach the analytic values shown in Table I. For the intermediate coupling region of $\lambda/U \sim 0.1$, $k_4(2,4)$ and $k_6(2,4)$ smoothly change between the LS and j - j coupling values. We note that $k_4(2,4) < 0$ and $k_6(2,4) < 0$, suggesting that the sign of $B_4^0(2,4)$ and $B_6^0(2,4)$ should be different from that of B_4^0 . In order to set $B_4^0(2,4) > 0$ and $B_6^0(2,4) > 0$ for the comparison with the results in Ref. 2, the sign of W is taken as negative.

Here we remark that $k_4(2,4)$ and $k_6(2,4)$ become good measures to show how the situation is close to the LS or the j - j coupling scheme. For actual materials, it is considered that U is about 1eV, while λ is in the order of 0.1 eV, leading to λ/U in the order of 0.1. From Figs. 2(c) and 2(d), $k_4(2,4)$ and $k_6(2,4)$ in such a region are close to neither the value of the LS nor that of the j - j coupling scheme. Namely, the actual situation corresponds to the intermediate coupling region. In particular, we note that the LS coupling scheme is different from the actual situation, in contrast to the naive expectation for the validity of the LS coupling scheme. One may consider that we can fit the results of the intermediate coupling region by changing $B_4^0(n, J)$ and $B_6^0(n, J)$ in the LS coupling scheme. It is true that we can change A_4 and A_6 as fitting parameters, but it is not allowed to fit the Stevens factors, which are determined by U and λ under the symmetry constraint. Thus, the actual situation of the intermediate coupling region is different both from the LS and j - j coupling schemes.

However, the above results on the smooth change of $B_4^0(2,4)$ and $B_6^0(2,4)$ seem to indicate that the LS and j - j coupling schemes are continuously connected. In fact, when we evaluate the overlap integral concerning the ground-state wavefunction, the magnitude is continuously changed between the LS and j - j coupling schemes. In Fig. 2(e), we show the overlap integral $\langle \Psi | \Psi_{j-} \rangle$ as a function of λ/U .

When we decrease λ/U , we find that the overlap integral is gradually decreased, but even at the limit of $U=\infty$, we still find $\langle \Psi_{LS} | \Psi_{j-j} \rangle = 0.865$. Namely, the f^2 -state composed of a couple of electrons in the $j=5/2$ sextet becomes the good approximation for the LS coupling scheme, even though the $j=7/2$ octet is simply discarded.

In principle, it is possible to approach the intermediate coupling region either from the LS or the $j-j$ coupling limit, as mentioned in Sec. 2.2. Depending on the nature of the problem, we can prefer one of them, but in this paper, the $j-j$ coupling scheme is chosen. Here we remark that $\langle \Psi | \Psi_{j-j} \rangle$ is close to unity in comparison with $\langle \Psi | \Psi_{LS} \rangle$ in the intermediate coupling region. In fact, for $\lambda/U=0.1$, we find $\langle \Psi | \Psi_{j-j} \rangle = 0.972$, while $\langle \Psi | \Psi_{LS} \rangle = 0.957$.

Now we discuss the results of H_{eff} . In Figs. 2(c) and 2(d), broken curves denote $k_4(2, 4)$ and $k_6(2, 4)$ evaluated from eq. (44), respectively. We clearly observe that the results are actually improved from the values of the $j-j$ coupling limit. In addition, it is found that they are close to the solid curves even for λ/U in the order of 0.1, i.e., in the intermediate coupling region. This fact supports the previous statement that H_{eff} works even for λ in the order of 0.1 eV, when we take U in the order of eV.

In Fig. 2(f), we show the energy levels of H_{eff} by black solid curves for $\lambda=0.2$ eV and $U=1$ eV. For comparison, we show the results of H by red broken curves for the same parameters. Note that we directly diagonalize H_{eff} and H to depict solid and broken curves. In the first impression, the results of H_{eff} are similar to those of H . Since the effect of B_6^0 is now included efficiently in the effective interaction eq. (31), the CEF energy levels of H are well reproduced. In particular, we can obtain Γ_3^+ doublet ground state, which does not appear in the limit of $\lambda=\infty$.

Although we do not have perfect agreements between the results of H_{eff} and H in Fig. 2(f), it should be noted that we do not adjust any parameters. In this sense, it is concluded that the characteristic features of the CEF energy levels of H are well captured by H_{eff} . Readers may consider that it is possible to fit the results of H by the LS coupling scheme due to the adjustment of the CEF parameters. However, the adjustable parameters, A_4 and A_6 in eqs. (33), are considered to depend on materials, not on U and λ . As remarked above, we cannot adjust the ratios of the Stevens factors, $k_4(n, J)$ and $k_6(n, J)$, since they are determined by the symmetry requirement and the values of U and λ . Namely, the difference in the intermediate coupling region between the original Hamiltonian H and the LS coupling scheme cannot be improved essentially, as long as we consider the limit of $U=\infty$. If we actually intend to improve the LS coupling scheme, it is necessary to consider, for instance, the expansion in terms of $1/U$ from the limit of $U=\infty$. This is an alternative way to construct the effective model in the intermediate coupling region.

3.2 f^3 states

Next we consider the case of $n=3$ by following the same discussion flow as in the previous subsection for $n=2$. In Figs. 3(a) and 3(b), we show the CEF energy levels obtained by the direct diagonalization of H for $(U, \lambda)=(10^5, 1)$ and $(1, 10^5)$, respectively. In the LS coupling scheme, the ground state multiplet is characterized by ${}^4I_{9/2}$ ($L=6, S=3/2, J=9/2$).

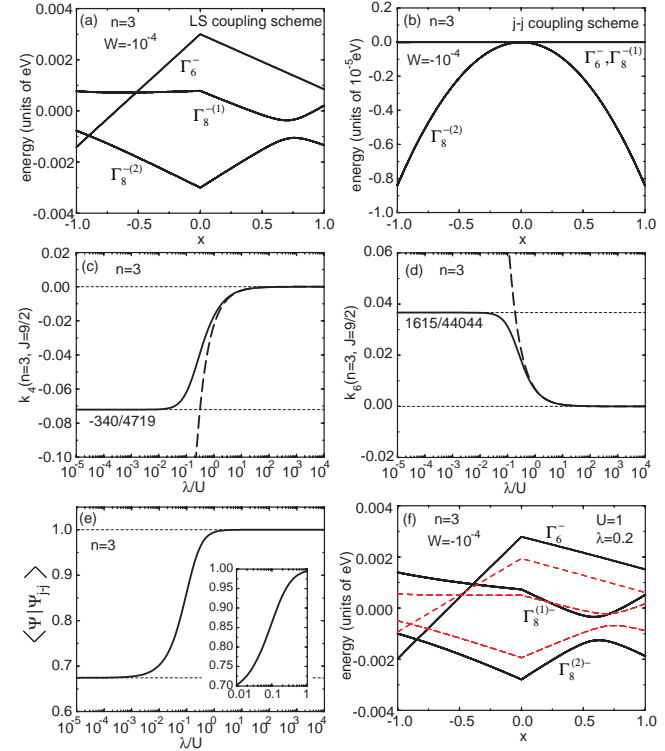


Fig. 3. CEF energy levels (a) in the LS coupling and (b) the $j-j$ coupling schemes for $n=3$. To express virtually the LS and $j-j$ coupling schemes, we set $(U, \lambda)=(10^5, 1)$ and $(1, 10^5)$ for H in (a) and (b), respectively. (c) $k_4(3, 9/2)$ and (d) $k_6(3, 9/2)$ as functions of λ/U for $n=3$. Broken curves denote $k_4(3, 9/2)$ and $k_6(3, 9/2)$ evaluated from H_{eff} . (e) Overlap integral $\langle \Psi | \Psi_{j-j} \rangle$ as functions of λ/U for $n=3$. Inset indicates the result in the intermediate coupling region in a magnified scale. (f) CEF energy levels of H_{eff} (black solid curves) and H (red broken curves) for $n=3, U=1$, and $\lambda=0.2$.

The 10-fold degenerate state is split into two Γ_8^- and one Γ_6^- states under the Cubic CEF.² On the other hand, in the limit of the $j-j$ coupling scheme, the situation seems quite different. As shown in Fig. 3(b), the Γ_6^- quartet always becomes the ground state, while the energy for the 6-fold degenerate excited states including another Γ_8^- quartet and Γ_6^- doublet do not depend on the CEF potential. We find that the curve for the ground state quartet is quadratic in terms of the CEF potential, suggesting that the contribution in the order of W vanishes in the limit of the $j-j$ coupling scheme, as suggested from $k_4^{j-j}(3, 9/2)=k_6^{j-j}(3, 9/2)=0$. Namely, the Stevens Hamiltonian H_S does not work in this case. However, it is found that the results of $H_a^{(0)}$ for $n=3$ correctly reproduce the CEF energy levels in Fig. 3(b). This fact clearly indicates that it is necessary to calculate the energy levels by diagonalizing simultaneously the Coulomb interaction and the CEF potential terms in the $j-j$ coupling scheme. As already mentioned, we always perform the direct diagonalization of H_{eff} in the $j-j$ coupling scheme. The Stevens Hamiltonian in the $j-j$ coupling scheme is used only for the purpose to estimate $k_4(n, J)$ and $k_6(n, J)$.

Figures 3(c) and 3(d) denote $k_4(3, 9/2)$ and $k_6(3, 9/2)$, respectively. We find that the values at the limits of $U=\infty$ and $\lambda=\infty$ are exactly the same as the analytic values in the LS and $j-j$ coupling schemes (see Table. I). In particular, we confirm that $k_4^{j-j}(3, 9/2)=k_6^{j-j}(3, 9/2)=0$, consistent with the

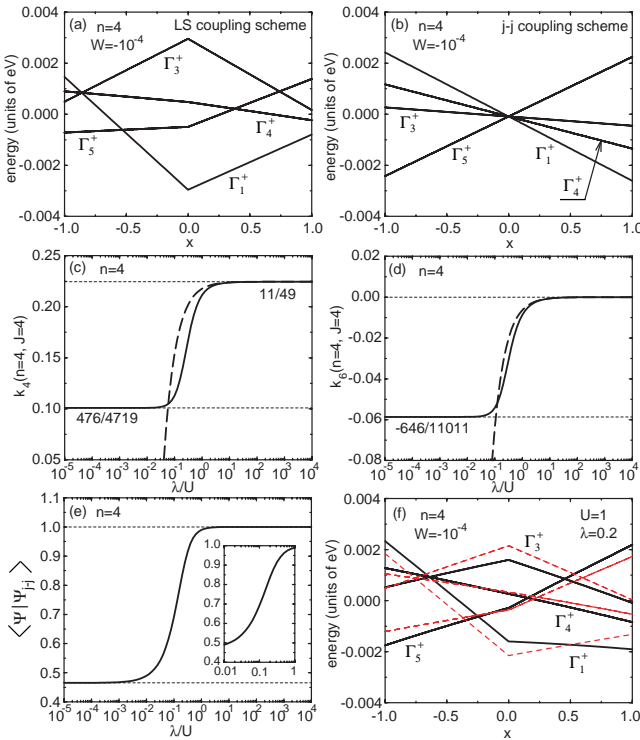


Fig. 4. (a) CEF energy levels in the LS coupling scheme for $n=4$, obtained by diagonalizing H for $U=10^5$ and $\lambda=1$. (b) CEF energy levels in the $j\text{-}j$ coupling scheme for $n=4$. Here we set $U=1$ and $\lambda=10^5$ for H . (c) $k_4(4, 4)$ and (d) $k_6(4, 4)$ as functions of λ/U for $n=4$. Broken curves denote $k_4(4, 4)$ and $k_6(4, 4)$ evaluated from H_{eff} . (e) Overlap integral $\langle \Psi | \Psi_{j-j} \rangle$ as functions of λ/U for $n=4$. Inset indicates the result in the intermediate coupling region in a magnified scale. Inset shows the result in the intermediate coupling region. (f) CEF energy levels of H_{eff} (black solid curves) and H (red broken curves) for $n=4$, $U=1$, and $\lambda=0.2$.

quadratic behavior of the CEF energy in Fig. 3(b). In Fig. 3(e), we depict the overlap integral as a function of λ/U . When we decrease λ/U , the overlap integral is decreased and at the limit of $U=\infty$, we find $\langle \Psi_{LS} | \Psi_{j-j} \rangle = 0.674$. It seems to be larger than we have naively expected. In the intermediate coupling region, we find $\langle \Psi | \Psi_{j-j} \rangle = 0.862$ for $\lambda/U=0.1$ and $\langle \Psi | \Psi_{j-j} \rangle = 0.932$ for $\lambda/U=0.2$. These results indicate that it is meaningful to construct the f^3 -electron state only by using the $j=5/2$ sextet in the intermediate coupling region for $n=3$.

In Figs. 3(c) and 3(d), we also show $k_4(3, 9/2)$ and $k_6(3, 9/2)$ evaluated from eq. (44) by broken curves. They deviate from the solid curves around at $\lambda \sim 1$, but as shown in Fig. 3(f), even for $\lambda=0.2$ and $U=1$, characteristic features of the CEF energy levels of H are reproduced by H_{eff} . Thus, in the same approximation level when we use the LS coupling scheme, we can exploit H_{eff} for the purpose to fit the experimental results by adjusting A_4 and A_6 in eqs. (33). There is an advantage of H_{eff} that the common CEF parameters can be used, even when the local f -electron number is changed. It is concluded that our modified $j\text{-}j$ coupling scheme works well to consider the multi- f -electron state.

3.3 f^4 states

Encouraged by the results of $n=2$ and 3, let us further proceed to the case of $n=4$. In Figs. 4(a) and 4(b), we show the CEF energy levels for $n=4$ obtained by the direct diagonalization of H for $(U, \lambda)=(10^5, 1)$ and $(1, 10^5)$, respectively. For

$n=4$, the ground state multiplet is characterized by 5I_4 ($L=6$, $S=2$, $J=4$). The nontet is split into Γ_1^+ singlet, Γ_3^+ doublet, and two kinds of triplets (Γ_4^+ and Γ_5^+).² Since the value of J for $n=4$ is equal to that of $n=2$, the CEF states are in common with Fig. 2(a), but the x dependence is different, since the sign of $k_4^{LS}(4, 4)$ is different from $k_4^{LS}(2, 4)$. Due to the same reason, we find that the x dependence of the CEF energy levels in Fig. 4(b) is reversed from that of Fig. 2(b) in the $j\text{-}j$ coupling scheme.

In Figs. 4(c) and 4(d), we show $k_4(4, 4)$ and $k_6(4, 4)$ by solid curves, indicating that the values in the LS and the $j\text{-}j$ coupling limits are correctly reproduced with the smooth changes between them. When we compare them with the results for $k_4(4, 4)$ and $k_6(4, 4)$ evaluated from eq. (44) (broken curves), they begin to deviate from the solid curves around at $\lambda=2\sim 3$. As shown in Fig. 4(e), at the limit of $U=\infty$, we obtain $\langle \Psi_{LS} | \Psi_{j-j} \rangle = 0.465$ for $n=4$. In the intermediate coupling region, we find $\langle \Psi | \Psi_{j-j} \rangle = 0.692$ for $\lambda/U=0.1$ and $\langle \Psi | \Psi_{j-j} \rangle = 0.836$ for $\lambda/U=0.2$. Even for $n=4$, in the intermediate coupling scheme, the ground state is well approximated by the $j\text{-}j$ coupling scheme. Then, it is still possible to reproduce the results in the intermediate coupling region. In fact, as shown in Fig. 4(f), the CEF energy levels of H look similar to those of H_{eff} for $U=1$ and $\lambda=0.2$.

3.4 f^5 states

Now we move on to the case of $n=5$. In Figs. 5(a) and 5(b), we depict the CEF energy levels due to the direct diagonalization of H with $n=5$ for $(U, \lambda)=(10^5, 1)$ and $(1, 10^5)$, respectively. For $n=5$, the ground state multiplet is characterized by $^6H_{5/2}$ ($L=3$, $S=5/2$, $J=5/2$). The sextet is split into Γ_7^- doublet and Γ_8^- quartet.²

Here readers may consider that the CEF energy levels for $n=5$ are simply the same as those in the case of $n=1$, but we should not simply conclude it. Namely, as easily understood from Figs. 5(a) and 5(b), the x dependence of the CEF energy levels is just reversed between the LS and $j\text{-}j$ coupling schemes. It should be noted that this phenomenon is *not* due to the approximation, but the intrinsic feature of the original Hamiltonian H . Note also that for $n=1$ and 5, the only relevant CEF parameter is $B_4(n, J)$, since the sixth-order CEF potential terms do not appear in the space of $J=5/2$. In the limit of the LS coupling scheme, since $k_4(5, 5/2)$ and $k_4(1, 5/2)$ have the same sign, the ground state character should not be changed between the cases of $n=1$ and 5.

On the other hand, in the limit of the $j\text{-}j$ coupling scheme, the x dependence of the CEF ground state of $n=5$ is reversed from that of $n=1$, since the sign of $k_4(5, 5/2)$ is different from that of $k_4(1, 5/2)$ in the $j\text{-}j$ coupling limit, as shown in Table I. We can understand the reason more intuitively from the electron-hole relation on the basis of the $j\text{-}j$ coupling scheme. Namely, to obtain the f^5 -electron state in the $j\text{-}j$ coupling scheme, we accommodate five electrons in the one-electron potential levels, for instance, such as Γ_7^- ground and Γ_8^- excited states for $B_4^0(1, 5/2) > 0$ ($x < 0$ and $W < 0$). Then, we obtain Γ_8^- ground and Γ_7^- excited states for the case of $n=5$ in the same region of x . In Fig. 5(c), we depict $k_4(5, 5/2)$ as a function of λ/U for $n=5$. We confirm that $k_4(5, 5/2)$ smoothly changes from $-11/7$ at $\lambda=\infty$ to $13/21$ at $U=\infty$.

When we compare the solid curves with the broken ones

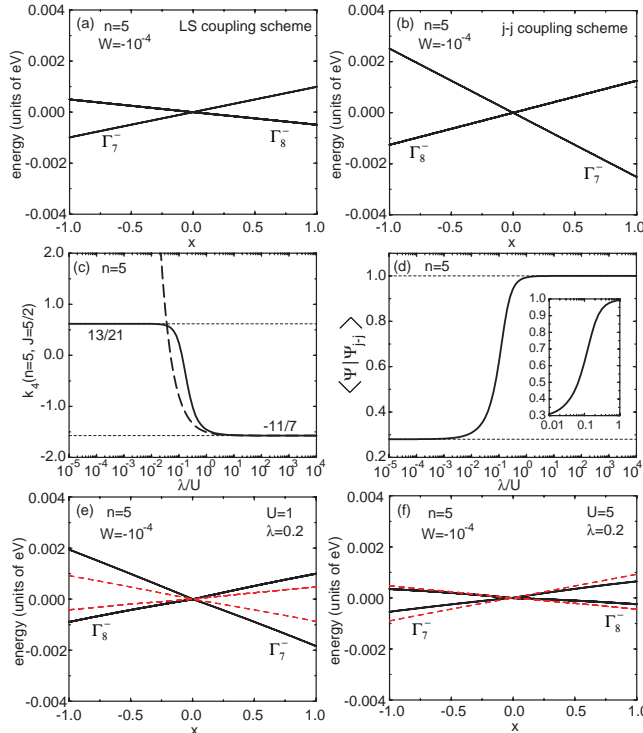


Fig. 5. (a) CEF energy levels in the *LS* coupling scheme for $n=5$. We diagonalize H for $U=10^5$ and $\lambda=1$. (b) CEF energy levels of H in the *j-j* coupling scheme for $n=5$. Here we set $U=1$ and $\lambda=10^5$. (c) $k_4(5, 5/2)$ as a function of λ/U for $n=5$. Broken curve denotes the result estimated from H_{eff} . (d) Overlap integral $\langle \Psi | \Psi_{j-j} \rangle$ as a function of λ/U for $n=5$. Inset denotes the result in the intermediate coupling region in a magnified scale. CEF energy levels of H_{eff} and H for (e) $U=1$ and (f) $U=5.5$ with $n=5$ and $\lambda=0.2$. In both figures, we depict the results of H_{eff} and H by black solid and red broken curves, respectively.

for $k_4(5, 5/2)$ estimated from eq. (44), the deviation begins to occur at λ between 1 and 10. Namely, the degree of approximation seems to be worse in comparison with the case of $n=4$. In fact, we obtain the smaller overlap integral for $n=5$, $\langle \Psi_{LS} | \Psi_{j-j} \rangle = 0.280$, as shown in Fig. 5(d). However, in the intermediate coupling region, we find $\langle \Psi | \Psi_{j-j} \rangle = 0.622$ at $\lambda=0.1$ and $\langle \Psi | \Psi_{j-j} \rangle = 0.857$ at $\lambda=0.2$, for a fixed value of $U=1$. At $\lambda=0.2$, $\langle \Psi | \Psi_{j-j} \rangle$ for $n=5$ is larger than that for $n=4$, as discussed in Sec. 2.2. In any case, the ground-state wavefunction in the intermediate coupling region is still approximated well by the states constructed from the *j-j* coupling scheme for $n=5$. We can reproduce the results of H by H_{eff} for $U=1$ and $U=5$ at $\lambda=0.2$, as shown in Figs. 5(e) and 5(f). In particular, in the effective model of H_{eff} , we can reproduce the interchange of the ground state, when we change the ratio of λ/U . Note, however, that we cannot quantitatively reproduce the critical value of U at which the ground states are interchanged.

In order to understand the interchange of the ground state for the case of $n=5$ within the *LS* coupling scheme, the only way is to change the sign of W phenomenologically, since $k_4^{LS}(5, 5/2)$ is fixed due to the symmetry requirement. However, in our modified *j-j* coupling scheme, we can consider the microscopic origin of the change of the CEF parameter due to the competition between the Coulomb interaction and the spin-orbit coupling. It is an advantage of our effec-

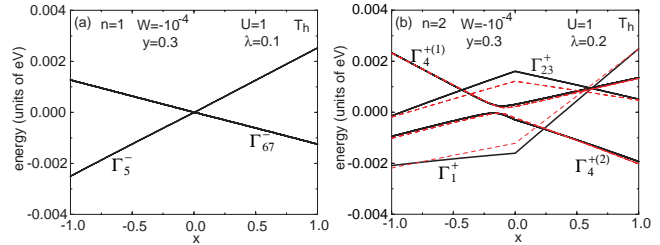


Fig. 6. CEF energy levels of H_{eff} (black solid curves) for (a) $n=1$ and (b) $n=2$ for T_h symmetry with $y=0.3$. The spin-orbit interaction is set as (a) $\lambda=0.1$ and (b) $\lambda=0.2$. In the panel (b), we also show the results of H by red broken curves for the same parameters.

tive model, in addition to the reproduction of the CEF energy levels of H .

As for the change of the sign in the CEF parameter, when we consider the different material groups, we may choose positive or negative W depending on the kind of materials. However, for the same material group with the same rare-earth ion, it is difficult to imagine that the sign of the CEF parameter is changed, although the magnitude may be different due to the change of ligand ions. Rather, as found in the present calculations, it seems natural to understand that the CEF ground state is converted due to the effect of the Coulomb interaction and/or the spin-orbit coupling. This is considered to explain a possible conversion of the CEF ground state in Sm-based filled skutterudites, as mentioned in the next subsection.

3.5 T_h symmetry

In order to show the effectiveness of our modified *j-j* coupling scheme, let us also discuss the CEF energy levels for filled skutterudites with T_h symmetry.^{28,29} For the purpose, it is necessary to add extra B_6^2 terms²² in $B_{m,m'}$ as⁹

$$\begin{aligned} B_{3,1} &= B_{-3,-1} = 24\sqrt{15}B_6^2, \\ B_{2,0} &= B_{-2,0} = -48\sqrt{15}B_6^2, \\ B_{1,-1} &= -B_{3,-3} = 360B_6^2. \end{aligned} \quad (45)$$

By following Ref. 22, we express B_6^2 as $B_6^2 = Wy/F^t(6)$ with $F^t(6) = 24$ for $J=3$. Here we set $y=0.3$ as a typical value for filled skutterudites.

In Figs. 6(a) and 6(b), we show the energy levels for $n=1$ and 2 by diagonalizing H_{eff} for $\lambda=0.1$ and 0.2, respectively, with $U=1$. For the case of $n=2$, we also depict the results of H by red broken curves. For $n=1$, we have Γ_5^- doublet and Γ_{67}^- quartet states, which are essentially the same as Γ_7^- doublet and Γ_8^- quartet for O_h symmetry. For $n=2$, we find remarkable difference from the case of O_h symmetry. As already mentioned in Ref. 22, two triplets Γ_4^+ and Γ_5^+ in O_h symmetry are mixed and they are $\Gamma_4^{+(1)}$ and $\Gamma_4^{+(2)}$ in T_h symmetry. It is found that the results of H in the intermediate coupling region are well reproduced by H_{eff} . It is quite natural, since the effect of B_6^2 is effectively included in H_{eff} . It is emphasized here that such a characteristic issue of T_h symmetry is correctly reproduced in our modified *j-j* coupling scheme.

For $n=5$, we have Γ_5^- (Γ_7^- in O_h) doublet and Γ_{67}^- (Γ_8^- in O_h) quartet states. Thus, the results are essentially the same as those in Figs. 5(e) and 5(f). As mentioned above, for Sm-based filled skutterudites, it has been recently pointed

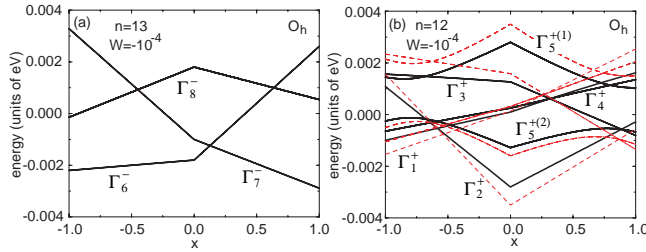


Fig. 7. CEF energy levels of $H_b^{(0)}$ (black solid curves) for (a) $n=13$ and (b) $n=12$ with $U=1$ and $W=-10^{-4}$. For comparison, in the panel (b), we also show the results of H in the LS coupling scheme ($U=10^5$ and $\lambda=1$) by red broken curves.

out a possibility that the ground states are changed between Γ_5^- doublet and Γ_{67}^- quartet. For $\text{SmRu}_4\text{P}_{12}$, $\text{SmOs}_4\text{P}_{12}$, and $\text{SmOs}_4\text{Sb}_{12}$, it has been considered that Γ_{67}^- quartet is the ground state.³⁰⁻³² On the other hand, for $\text{SmFe}_4\text{P}_{12}$, a possibility of Γ_5^- doublet ground state has been suggested.^{31,33} It can be interpreted that the conversion of the CEF ground state is due to the change of the Coulomb interaction and/or the spin-orbit coupling, which naturally leads to the change in the sign of B_6^0 . This point will be discussed in detail elsewhere with numerical results on the possible multipole state of Sm-based filled skutterudites.³⁴

4. Discussion and Summary

In this paper, we have proposed the effective model to consider systematically the multi- f -electron states by using the expansion in terms of $1/\lambda$. We have shown that the results in the intermediate coupling region for $n=2\sim 5$ can be reproduced well by the effective model and the applicability of the model has been clarified. The CEF state for T_h symmetry can be also reproduced.

We have stated that $H_a^{(0)}$ cannot reproduce even qualitatively the energy levels of the intermediate coupling region as well as the LS coupling scheme, since the effect of B_6^0 is not included. Here readers may have a question: If the effect of B_6^0 is included in the one-electron potential, does the zeroth-order term mimic the LS coupling results? The answer is yes. This can be clarified by considering the cases of $n=13$ and 12, i.e., the situations of one and two holes in the $j=7/2$ octet. For $j=7/2$, the zeroth-order term of $1/\lambda$ is given by

$$H_b^{(0)} = \sum_{\beta_1, \beta_2} \tilde{B}_{\beta_1, \beta_2}^{b, b} f_{\beta_1}^\dagger f_{\beta_2} + \sum_{\beta_1 \sim \beta_4} \tilde{I}_{\beta_1 \beta_2, \beta_3 \beta_4}^{bb, bb} f_{\beta_1}^\dagger f_{\beta_2}^\dagger f_{\beta_3} f_{\beta_4}, \quad (46)$$

where $\tilde{B}_{\beta_1, \beta_2}^{b, b}$ is given by the CEF potential for $j=7/2$ and $\tilde{I}_{\beta_1 \beta_2, \beta_3 \beta_4}^{bb, bb}$ is the Coulomb interaction among $j=7/2$ octet.

In Figs. 7(a) and 7(b), we show the energy levels of $H_b^{(0)}$ by black solid curves for $n_b=7$ and 6, corresponding to $n=13$ and 12, respectively, where $n_b=n-6$ and n_b denotes the electron number in the $j=7/2$ octet. Note that the results are obtained by the diagonalization of $H_b^{(0)}$. For comparison, for the case of $n=12$, we also show the results in the LS coupling scheme, by setting $U=10^5$ and $\lambda=1$ for H . In the $j=7/2$ octet, the effect of B_6^0 is already included in the one-hole case ($n=13$),

as easily understood from the Hutchings table for $J=7/2$. For the two-hole case ($n=12$), as shown in Fig. 7(b), even without considering the $1/\lambda$ -correction term $H_b^{(1)}$, the CEF energy levels of $H_b^{(0)}$ (black solid curves) are quite similar to those in the LS coupling scheme for $J=6$. Of course, in order to reproduce quantitatively the CEF energy levels in the realistic intermediate coupling region, it is necessary to include the terms in the order of $1/\lambda$ for the $j=7/2$ octet, as has done in this paper for the $j=5/2$ sextet. However, for practical purposes such as the fitting of experimental results, it seems enough to use $H_b^{(0)}$ for Tm and Yb compounds. When we further proceed to the cases of $n<12$, it is recommended to improve $H_b^{(0)}$ by considering the $1/\lambda$ corrections. It is one of future issues, when we attempt to develop a microscopic theory of magnetism in heavy rare-earth compounds.

As for a possible application of our modified $j\text{-}j$ coupling scheme, we consider a direction to improve effectively the band-structure calculations for f -electron materials. In the relativistic band-structure calculations, all the one-electron CEF potentials for $j=5/2$ and $7/2$ states are correctly included,³⁵ but the multi- f -electron state is not completely reproduced in comparison with the CEF levels of the LS coupling scheme. In order to construct the multi- f -electron state due to the one-electron basis, it is necessary to treat correctly the competition among Coulomb interactions, spin-orbit coupling, and CEF potentials, but in the band-structure calculations, the effect of Coulomb interactions, in particular, the Hund's-rule coupling, is considered only partly within the mean-field approximation. An effective way to improve such a situation is to include the two-body CEF potentials discussed here in the band-structure calculations with due care. It is one of future problems to develop a systematic way for the inclusion.

Another issue is the CEF effect on exotic itinerant magnetism and unconventional superconductivity of f -electron materials from the band picture. We can construct the appropriate many-body Hamiltonian for f -electron systems, by adding the hybridization term between f and conduction electrons or the hopping term of f electrons to the local f -electron term H_{eff} in the modified $j\text{-}j$ coupling scheme. The parameters in the kinetic term are determined so as to reproduce the energy bands near the Fermi level. It is another future problem to analyze such a model by using numerical and/or analytical techniques.

In summary, we have discussed the f^n -electron states with $n\geq 2$ on the basis of the effective model obtained by including the corrections in the order of $1/\lambda$ in the $j\text{-}j$ coupling scheme. For $n=2\sim 5$, the results in the realistic intermediate coupling region have been quantitatively reproduced in our modified $j\text{-}j$ coupling scheme. By using H_{eff} , we have also reproduced correctly the CEF energy levels for T_h symmetry. In conclusion, for the consideration of multi- f -electron states, we can use the $j\text{-}j$ coupling scheme with appropriate corrections in terms of $1/\lambda$.

Acknowledgment

The authors thank K. Kubo, H. Onishi, and K. Ueda for discussions and comments. This work was supported by a Grant-in-Aid for Scientific Research (C)(2) under the contract No. 16540316 from Japan Society for the Promotion of Sci-

ence (JSPS). We have been separately supported by Grant-in-Aids for Scientific Research in Priority Area “Skutterudites” under the contract Nos. 18027016 and 15072204 from the Ministry of Education, Culture, Sports, Science, and Technology of Japan. One of the authors (T.H.) has been also supported by a Grant-in-Aid for Scientific Research (C) under the contract No. 18540361 from JSPS. Part of the computation in this work has been done using the facilities of the Supercomputer Center of Institute for Solid State Physics, University of Tokyo.

- 1) K. W. H. Stevens: Proc. Phys. Soc. **A65** (1952) 209.
- 2) K. R. Lea, M. J. M. Leask and W. P. Wolf: J. Phys. Chem. Solids **23** (1962) 1381.
- 3) M. T. Hutchings: Solid State Phys. **16** (1964) 227.
- 4) T. Hotta and K. Ueda: Phys. Rev. B **67** (2003) 104518.
- 5) T. Hotta: Rep. Prog. Phys. **69** (2006) 2061.
- 6) T. Hotta: Phys. Rev. B **70** (2004) 054405.
- 7) H. Onishi and T. Hotta: New J. Phys. **6** (2004) 193.
- 8) T. Hotta: Phys. Rev. Lett. **94** (2005) 067003.
- 9) T. Hotta: J. Phys. Soc. Jpn. **74** (2005) 1275.
- 10) T. Takimoto, T. Hotta, T. Maehira and K. Ueda: J. Phys.: Condens. Matter **14** (2002) L369.
- 11) T. Takimoto, T. Hotta and K. Ueda: J. Phys.: Condens. Matter. **15** (2003) S2087.
- 12) T. Takimoto, T. Hotta and K. Ueda: Phys. Rev. B **69** (2004) 104504.
- 13) T. Hotta and K. Ueda: Phys. Rev. Lett. **92** (2004) 107007.
- 14) K. Kubo and T. Hotta: J. Phys. Soc. Jpn. **75** (2006) 083702.
- 15) K. Kubo and T. Hotta: J. Phys. Soc. Jpn. **75** Suppl. (2006) 232.
- 16) K. Kubo and T. Hotta: Phys. Rev. B **71** (2005) 140404(R).
- 17) K. Kubo and T. Hotta: Phys. Rev. B **72** (2005) 144401.
- 18) K. Kubo and T. Hotta: Phys. Rev. B **72** (2005) 132411.
- 19) T. Hotta: J. Phys. Soc. Jpn. **74** (2005) 2425.
- 20) T. Hotta: Phys. Rev. Lett. **96** (2006) 197201.
- 21) H. Onishi and T. Hotta: J. Phys. Soc. Jpn. **75** Suppl. (2006) 266.
- 22) K. Takegahara, H. Harima and A. Yanase: J. Phys. Soc. Jpn. **70** (2001) 1190; *ibid.* **70** (2001) 3468; *ibid.* **71** (2002) 372.
- 23) J. C. Slater: Phys. Rev. **34** (1929) 1293.
- 24) E. U. Condon and G. H. Shortley: Phys. Rev. **37** (1931) 1025.
- 25) J. A. Gaunt: Phil. Trans. Roy. Soc. **A228** (1929) 195.
- 26) G. Racah: Phys. Rev. **62** (1942) 438.
- 27) J. C. Slater: *Theory of Atomic Structure*, (McGraw-Hill, 1960).
- 28) H. Sato, H. Sugawara, T. Namiki, S. R. Saha, S. Osaki, T. D. Matsuda, Y. Aoki, Y. Inada, H. Shishido, R. Settai and Y. Ōnuki: J. Phys.: Condens. Matter **15** (2002) S2063.
- 29) Y. Aoki, H. Sugawara, H. Harima and H. Sato: J. Phys. Soc. Jpn. **74** (2005) 209.
- 30) S. Sanada, Y. Aoki, H. Aoki, A. Tsuchiya, D. Kikuchi, H. Sugawara and H. Sato: J. Phys. Soc. Jpn. **74** (2005) 246.
- 31) K. Matsuhira, Y. Doi, M. Wakeshima, Y. Hinatsu, H. Amitsuka, Y. Shimaya, R. Giri, C. Sekine and I. Shirotan: J. Phys. Soc. Jpn. **74** (2005) 1030.
- 32) Y. Aoki, S. Sanada, H. Aoki, D. Kikuchi, H. Sugawara and H. Sato: Physica B **378-380** (2006) 54.
- 33) Y. Nakanishi, T. Tanizawa, T. Fujino, H. Sugawara, D. Kikuchi, H. Sato and M. Yoshizawa: J. Phys. Soc. Jpn. **75** Suppl. (2006) 192.
- 34) T. Hotta: preprint.
- 35) H. Harima: J. Magn. Magn. Mater. **226-230** (2001) 83.